

The Analysis of a Heat Treated E110 Case Hardening Steel

K.V.S.Sruthi¹, Dr.K.Harinarayana²

¹Assistant professor in Professor, Department of Mechanical Engineering, CMR Engineering College

² Professor, Department of Mechanical Engineering, CMR Engineering College

ABSTRACT: This paper investigates mechanical and microstructural behaviour of E110 case hardening steel when subjected to different heat treatment processes including quenching, normalizing and tempering. After heat treatment samples were subjected to mechanical and metallographic analysis and the properties obtained from applying different processes were analysed. The heat treatment process had certain effects on the resultant properties and microstructures obtained for E110 steel which are described in details. Quenching produced a martensitic microstructure characterized by significant increase in material's hardness and a significant decrease in its impact energy. Annealed specimens produced a coarse pearlitic microstructure with minimal variation in hardness and impact energy. For normalized samples, fine pearlitic microstructure was identified with a moderate increase in hardness and significant reduction in impact energy. Tempering had a significant effect on quenched specimens, with a substantial rise in material ductility and reduction of hardness with increasing tempering temperature. Furthermore, Results provide additional substantiation of temper embrittlement theory for low-carbon alloys, and indicate potential occurrence of temper embrittlement for fine pearlitic microstructures.

Keywords: Heat treatment, Low carbon steel, Microstructure, Mechanical properties.

I. INTRODUCTION

Ever since its discovery in the Iron Age [1] steel has been one of the most widely employed materials known to mankind. It is essentially an alloy of iron and carbon, with a carbon content that typically varies between 0.05% and 2.1% [2]. Whilst iron provides mechanical properties that make it ductile and tough, carbon content determines the material's hardness. As a result, it is entirely possible to tailor the composition of a steel to suit a desired design purpose. Whilst steels are primarily classified by carbon content, they are frequently alloyed with a number of elements to further modify mechanical and chemical properties. Where total alloying element content is below 4%, the material is considered as a low alloy steel [3].

E110 steel (also known as 17CrNiMo6) is classified as a low carbon, high strength low alloy case hardening steel that combines core toughness and high case hardness following heat treatment. Its typical applications are in components with large cross sections that require high toughness and core strength, such as crankshafts, gears, and gear shafts in the aviation and automobile industry [4]. The typical composition of E110 steel in weight percent include 0.18 C, 0.30 Si, 0.50 Mn, 1.50 Ni, 1.70 Cr, 0.30 Mo, 0.025 S, and 0.025 P. Heat treatment of E110 steel is typically performed through case hardening processes during which the steel is heated in a carbon-rich environment to enable carbide absorption, followed by a quenching procedure. Numerous investigations have been conducted into mechanical properties and microstructure variations as a result of carburizing methods. Studies by Wang et al [5-8] have examined changes in core hardness, strength and toughness of carburized and quenched E110 steel, with significant physical and microstructural effects being recorded as a result of the introduction of carburized outer layer for the alloy. Extremely limited research, however, has been conducted on the effects of more traditional, non-carburizing approaches to heat treatment for E110. While case-hardening methods appear to be commonplace for this particular alloy, conventional processes of quenching, annealing, normalizing and tempering may provide different mechanical properties allowing the material to be employed across a wider range of applications.

This study investigates the influences of heat treatment processes on mechanical properties on mechanical properties and microstructural arrangement in E110 steel alloy.

II. PROCEDURE

Samples were made in compliance with ASTM A370 and EUROPEAN EN 10045 standards for Charpy-V impact specimens. Each “A”-, “N”- and “Q”-identified sample was subjected to a primary austenitization process to enable full gamma-phase transformation. To achieve this all samples were soaked above E110’s eutectoid temperature (approximately 880°C) for half an hour. Austenitization was optimized through selection of 900°C kiln temperature and, due to the relatively small specimen size, it was expected that 30 minutes soaking time would be sufficient to transform all samples’ microstructure into gamma phase configuration. Following the austenitization process, samples were cooled down depending on their alphabetical identifiers as presented in Table 1.

Samples with an “N”-identifier were removed from the kiln and placed on an open-air iron rack for air-cooled normalization to room temperature. All samples with a “Q”-identifier were removed from the kiln and water-quenched to room-temperature. All samples with an “A”-identifier were left inside the deactivated kiln to be furnace cooled to room temperature over a 24 hour period. Then all samples were subjected to mechanical testing in order to investigate variations in specimen impact energy and hardness with the different heat treatment processes employed.

TABLE 1. Specimen Identification.

Identifier	Description
S	As supplied
A	Annealed Untempered
A1	Annealed & Tempered at 100°C
A2	Annealed & Tempered at 200°C
A3	Annealed & Tempered at 300°C
A4	Annealed & Tempered at 400°C
A5	Annealed & Tempered at 500°C
A6	Annealed & Tempered at 600°C
N	Normalized Untempered
N1	Normalized & Tempered at 100°C
N2	Normalized & Tempered at 200°C
N3	Normalized & Tempered at 300°C
N4	Normalized & Tempered at 400°C
N5	Normalized & Tempered at 500°C
N6	Normalized & Tempered at 600°C
Q	Quenched Untempered
Q1	Quenched & Tempered at 100°C
Q2	Quenched & Tempered at 200°C
Q3	Quenched & Tempered at 300°C
Q4	Quenched & Tempered at 400°C
Q5	Quenched & Tempered at 500°C
Q6	Quenched & Tempered at 600°C

Charpy V-notch impact energy testing was performed using a Brooks Universal Pendulum Impact Tester Model IT3U for metals and alloys.. Then the hardness testing was performed using a Wolpert Universal Tester 751 using a diamond indenter, 60 kgf total load and scale calibrated to the Rockwell-A band. Results are tabulated in Table 2.

Reference samples, and specimens displaying high or low impact energy and hardness values, were prepared for optical surface metallography. The following samples were identified for investigation: S, A, A3, A4, A6, N3, N4, N5, Q2, Q4 and Q6. Then segment was cut from selected specimens using a Struers Labotom-3 powerful manual cut-off machine. Segments were mounted in Struers MultiFast thermosetting bakelite resin using a Struers CitoPress-1 automatic mounting press. Each sample was subjected to two grinding and one polishing process on a Struers LaboPol-25 coupled with a LaboForce-1 specimen mover and LaboDoser abrasive dosing unit. Grinding and polishing settings employed for each stage. Then etching was performed to introduce controlled corrosion to specimen surfaces in order to make microstructural composition readily identifiable. Each specimen was etched by a 1-2 second application of an etching agent to its surface. The etching agent consisted of Nitral prepared in-house of 5:1 ethanol and nitric acid composition. Metallographic samples were investigated under a Zeiss Axio Lab.A1 binocular microscope at 100x, 500x and 1000x optical magnification. Images were obtained through an AxioCam ERc5s module used in conjunction with Zeiss Zen 2011 software.

TABLE 2. Charpy-V Impact Energy and HRA Raw Data.

Identifier (from Table 3)	T _{temp} (°C)	HRA 1	HRA 2	HRA 3	HRA Avg.	CVN Impact Energy (J)
S	0	50.3	51.1	50.2	50.5	230
A	0	49.2	46.2	51.5	49.0	214
A1	100	51.9	46.7	52.5	50.4	204
A2	200	48.1	49.2	52.8	50.0	212
A3	300	51.5	51.5	51.3	51.4	217
A4	400	43.0	49.3	48.0	46.8	220
A5	500	45.5	47.3	47.2	46.7	202
A6	600	45.1	49.9	41.6	45.5	196
N	0	52.8	56.9	50.9	53.5	184
N1	100	54.2	57.5	57.3	56.3	186
N2	200	58.4	55.7	56.2	56.8	194
N3	300	50.4	52.1	52.3	51.6	202
N4	400	51.6	51.3	54.3	52.4	170
N5	500	53.9	52.0	53.1	53.0	204
N6	600	34.1	39.3	30.5	34.6	198
Q	0	63.8	65.7	63.2	64.2	172
Q1	100	65.0	59.8	66.2	63.7	175
Q2	200	61.0	57.6	59.2	59.3	202
Q3	300	61.6	67.7	57.0	62.1	176
Q4	400	60.5	58.6	59.5	59.5	163
Q5	500	56.2	47.6	46.0	49.9	202
Q6	600	48.4	47.6	46.0	47.3	300

III. RESULTS AND DISCUSSION

The mean hardness variation of heat treated samples from the untreated sample (S) has been -3.9%, 1.3% and 14.8% respectively for A, N and Q samples. Accordingly, the mean CVN impact energy variation of heat treated samples from the untreated sample (S) have been -9%, -16.9% and -13.7% respectively for A, N and Q samples which is in relative agreement with hardness values recorded.

Fig. 1 illustrates the microstructures obtained for the samples using an optical microscope. Fig. 1(a) shows the microstructure of quenched untempered specimen. The needle-shaped granular arrangement of the sample is consistent with a martensitic microstructure where the dark areas are the carbon-rich martensite phase and the white regions consist of retained austenite that failed to transform during the rapid cooling. Fig. 1(b) shows the microstructure obtained for the annealed untempered specimen. The microstructure indicates that annealing resulted in a large α -ferrite grain growth, represented by the white areas, with carbide deposits primarily occurring at grain boundaries and as occasional intergranular defects. It is presumed that the visible carbide deposits represent a coarse pearlitic phase although precise determination of lamellar cementite/ γ -ferrite structure is not possible without further magnification. Furthermore, pearlite colonies appear to exist in a vastly dominating primary α -ferrite phase. Microstructure of the normalized untempered specimen is shown in Fig. 1(c). The image indicates that normalizing resulted in a primary α -ferrite phase indicated by white regions, with a finely dispersed carbide phase throughout. It is presumed that the carbide phase consists of fine pearlite, although anticipated lamellar cementite/ γ -ferrite phases are indistinguishable at the provided levels of magnification. Furthermore, microstructural grain size appears to be significantly smaller than that observed in annealed specimens.

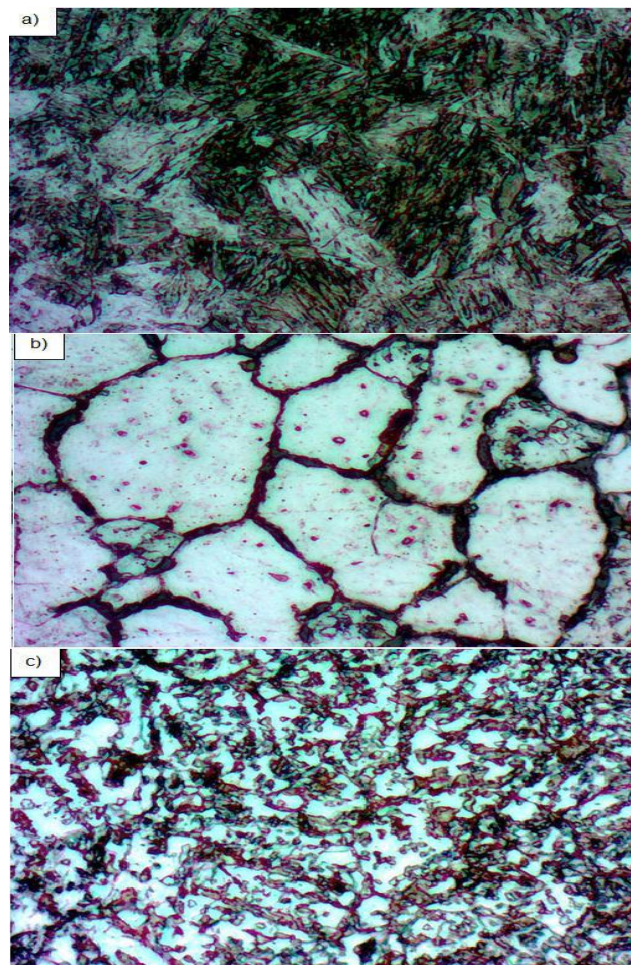


Fig. 1. Microstructures of Quenched (a), Annealed (b), and Normalized (c) Specimens at 1000x Magnification.

Fig. 2 displays the effect of tempering at on the microstructures of annealed samples. It appears that there was no significant modification to specimen microstructure due to tempering. A minor reduction in carbide content may be observed for the specimen tempered at 400°C shown in Fig. 2(c). Whilst a seemingly larger amount of dark areas can be observed in the microstructure of the 500°C tempered sample as shown in Fig. 2(d). This is mostly due to over-etching during specimen preparation.

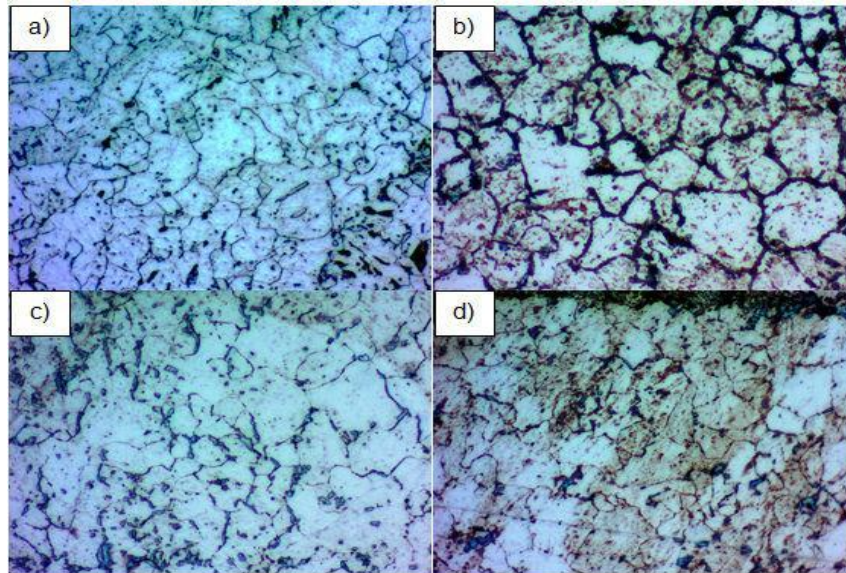


Fig. 2. Microstructures at 1000x Magnification of Annealed (a) Untempered and Tempered Specimens at (b) 300, (c) 400 and (d) 500°C.

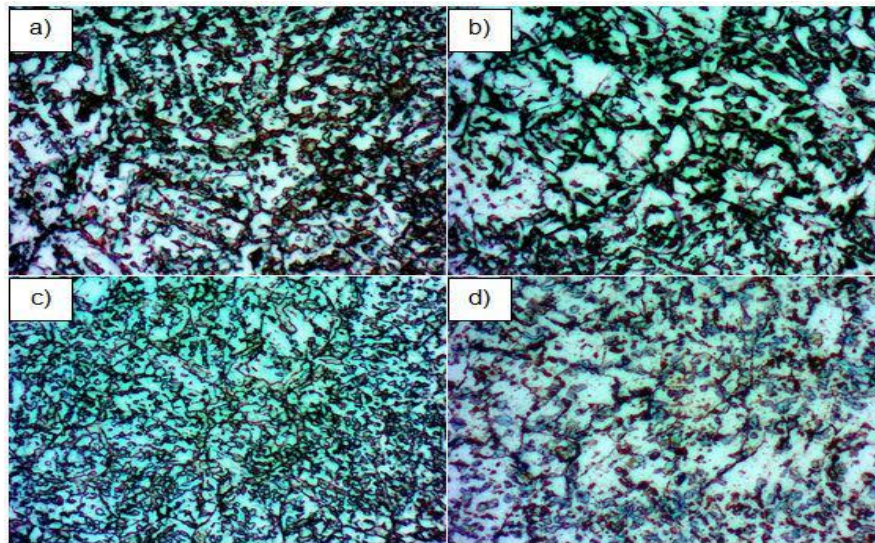
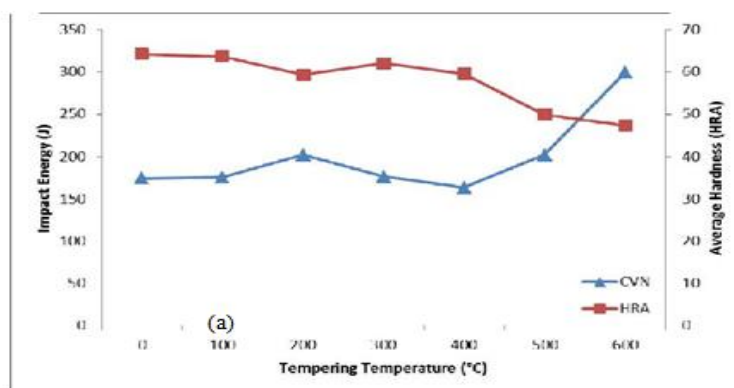


Fig. 3. Microstructures at 1000x Magnification of Normalized (a) Untempered and Tempered Specimens at (b) 300, (c) 400 and (d) 600°C.



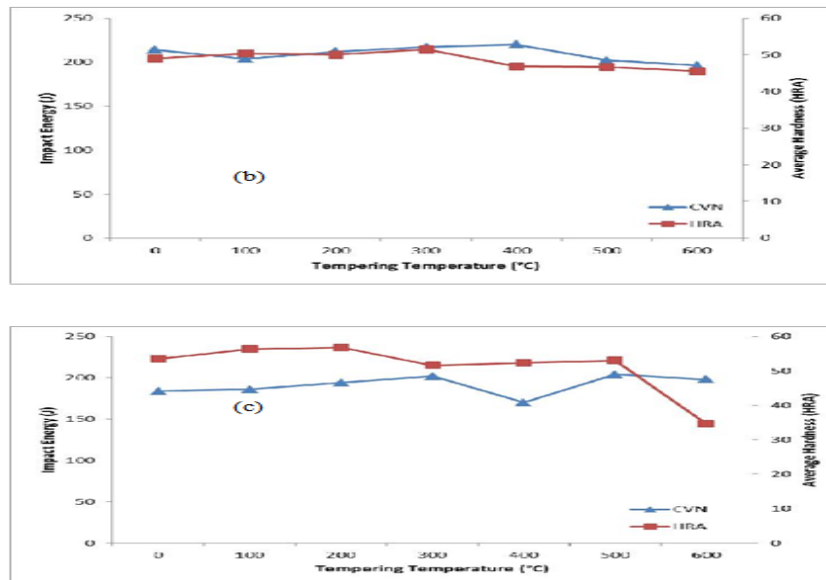


Fig. 4. Variation in Impact Energy and Average Hardness for Quenched (a), Annealed (b) and Normalized (c) Specimens.

The effects of tempering on the microstructure of normalized specimens are illustrated in Fig. 3. Whilst there is little variation in microstructure of the untempered specimen, Fig. 3(a), and the sample tempered at 300°C, Fig. 3(b); tempering at 400°C, Fig. 3(c) appears to have resulted in a finer level of carbide dispersion within the ferrite phase. Furthermore, following tempering at 600°C, 3(d), specimen microstructure contains a ferrite phase of similar concentration to the 300°C tempered specimen, however with less amounts of visible pearlite.

Fig. 4 displays variations in impact energy and average hardness for quenched, annealed and normalized samples subjected to tempering at different temperatures. For the quenched sample shown in Fig. 4(a) there was an overall inverse trend between hardness and tempering temperature, with maximum HRA (64) occurring for the untempered specimen and minimum HRA (47) observed for the sample tempered at 600°C. In most cases, hardness decreased with an increase in tempering temperature, except for 300°C, where a 5% rise in HRA was observed. For the annealed sample shown in Fig. 4(b) hardness values remained relatively constant with changes in tempering temperature, with maximum HRA (47) occurring for the specimen tempered at 300°C and minimum hardness (46) identified following tempering at 600°C. Generally, hardness was not significantly affected by tempering, with an average hardness reduction of 1% with respect to the annealed and untempered sample, and the largest HRA reduction of 7% occurring at 600°C. In the case of normalized sample shown in Fig. 4(c) hardness remained relatively constant up to tempering temperatures of 500°C with a hardness variation of up to 6%. A sudden decrease in hardness is observed for the specimen tempered at 600°C, resulting in a hardness drop of 35% with respect to the untempered specimen. This could be associated with spheroidite-like carbide decomposition due to stage four tempering previously identified in the literature and results are consistent with the findings in other researches [9, 10].

Fig. 5(a) displays variation in average hardness for all samples subjected to tempering at different temperatures. Overall, heat treatment procedures increased sample hardness for 14 from 21 cases, with an average HRA rise of 15% across all specimens. The largest increase in hardness was observed for the quenched untempered specimen, with an HRA rise of 27%. Whilst quenching and normalizing procedures increased hardness, annealing caused a minor decrease of 3% in the untempered state. For all specimens, a general inverse trend between hardness and tempering temperature was observed, with minimum HRA identified for the normalized sample following tempering at 600°C. Accordingly Fig. 5(b) shows the variation in impact energy for all samples subjected to tempering at different temperatures. Tempering temperature appears to have had a large effect on impact energy for quenched samples, but there is little to no correlation for annealed and normalized specimens. Whilst impact energy varied up to 74% for the quenched and 600°C tempered sample with respect to its untempered counterpart, overall variation across all samples only indicated an average of 6% difference to the untreated specimen. Annealed samples maintained relatively constant impact energy values across all tempering temperatures investigated. Normalized specimens likewise showed little variation, despite a drop of impact energy observed at 400°C.

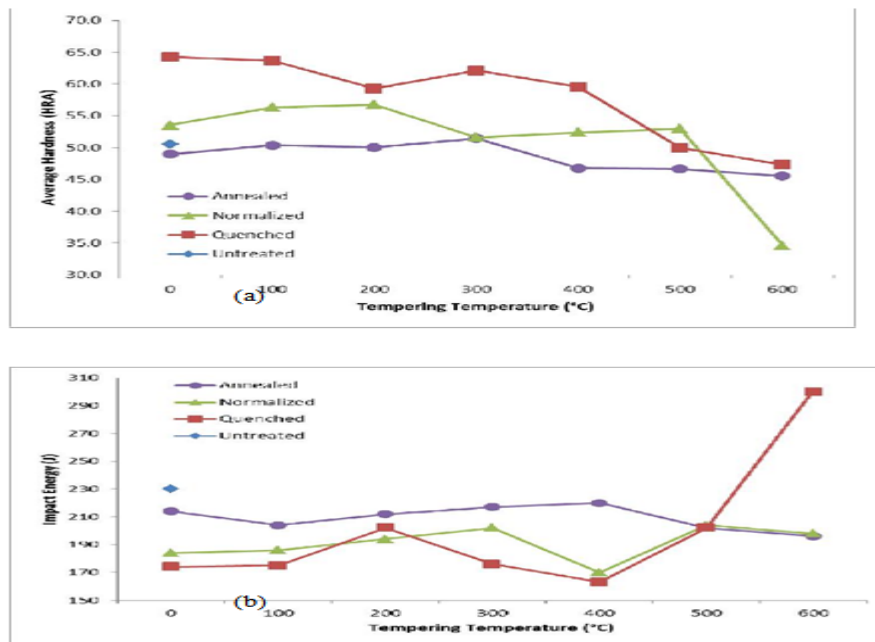


Fig. 5. Variation in Average Hardness and Impact Energy with Tempering Temperature for all Specimens.

IV. CONCLUSIONS

Results of the experiments performed suggest that E110 steels are prone to significant temper embrittlement following quenching processes. The data presented within this paper indicate potential temper embrittlement phenomena for normalized specimens upon exposure to temperatures around 400°C.

The quenching of the specimens produced a martensitic microstructure with significant increases in hardness and decreases in impact energy. Upon tempering, quenched samples experienced progressive martensite degradation into a dispersed carbide microstructure resulting in overall increases in impact energy and decreases in hardness. Furthermore, the general rise in material ductility was significantly higher than the corresponding drop in hardness, which indicates that tempering is a viable method of improving E110 toughness and workability without causing equal degradation to hardness. The results additionally indicate that quenched E110 steel is significantly prone to temper embrittlement between 300°C and 400°C, where a 20% reduction in the impact energy was observed.

The annealing of E110 specimens resulted in a large-grained highly ferritic coarse pearlite microstructure which is consistent with the relatively high impact energy and low hardness values obtained during mechanical testing. Due to the high presence of α -ferrite, the material takes on the ductile and soft properties associated with the vast iron phase. Tempering of annealed samples caused little change in microstructure and mechanical performance. There was a minor variation in material hardness and impact energy following tempering at 400°C which appears to be representative of the slightly higher ferritic microstructure observed for that sample. Normalizing of E110 specimens produced a fine pearlite microstructure of significantly smaller grain size than annealed specimens, resulting in moderate hardness and low ductility. The large variation in ductility caused by the normalizing process was attributed to significantly reduced grain size resulting in a decrease of grain boundary sliding mechanisms. Tempering of normalized samples resulted in overall hardness reduction, most significantly observed following tempering at 600°C due to carbide decomposition through stage four tempering. Sample ductility remained relatively constant except for an observed decrease in ductility after tempering at 400°C, which may be evidence to suggest temper embrittlement in coarse pearlitic microstructures.

REFERENCES

- [1]. Wagner, D.B. (2014). Early iron in India, Sri Lanka, China, Korea and Japan. Retrieved October 5, 2014, from <http://www.staff.hum.ku.dk>.
- [2]. Callister, W.D.; and Rethwisch, D.G. (2014). *Materials science and engineering: An introduction*. 9th Edition, John Wiley & Sons.
- [3]. Smith, W.F.; and Hashemi, J. (2009), *Foundations of materials science and engineering*, McGraw-Hill.
- [4]. Bohler Uddeholm Australia (2015). Case hardening steel. Retrieved March 12, 2015 from <http://www.buau.com.au/case-hardening-steel.php>

- [5]. Gao, J.-Z.; Wang, A.-X.; Gu, M.; Xu, H.-X. (2010). Study on the case hardenability of new type high-alloy carburizing gear steel. *Development and Application of Materials*, 5, 20-22, 26.
- [6]. Li, B.-K.; Wang, A.-X.; Zhao, S.-F.; Gu, M.; and Zhu, Q.-Y. (2007). Study on the distortion characteristic of 17CrNiMo6 steel during carburizing and hardening process and its control. *Heat Treatment Technology and Equipment*, 2, 36-38, 43.
- [7]. Wang, A.-X.; Gao, J.-Z., and Gu, M. (2010). Heat treatment of new type high alloy carburizing gear steel 17CrNiMo6. *Jinshu Rechuli / Heat Treatment of Metals*, 35(10), 82-86.
- [8]. Wang, C.; Wang, M.; Shi, J.; Hui, W.; and Dong, H. (2007). Effect of microstructure refinement on the strength and toughness of low alloy martensitic steel. *Journal of Materials Science and Technology (JMST)*, 23(5), 659-664.
- [9]. Kolahi-Aval, J.; and Mintz, B. (1989). Influence of tempering on impact behaviour of normalized steels. *Materials science and technology*, 5(5), 457-464.
- [10]. Altaweel, A.; and Tolouei-Rad, M. (2014). Effect of quenching media, specimen size and shape on the hardenability of AISI 4140 steel. *Emirates Journal for Engineering Research (EJER)*, 19(2), 33-39.